

Electronic structure of plutonium monochalcogenides

P. M. Oppeneer* and T. Kraft

Institute of Theoretical Physics, University of Technology, D-01062 Dresden, Germany

M. S. S. Brooks

European Commission, Joint Research Center, Institute for Transuranium Elements, D-76125 Karlsruhe, Germany

(Received 21 April 1999; revised manuscript received 2 September 1999)

The anomalous properties of the Pu monochalcogenides are investigated on the basis of electronic structure calculations. The Pu monochalcogenides are calculated to be semimetallic because, first the large spin-orbit interaction of the Pu $5f$ states splits the $5f_{5/2}$ and $5f_{7/2}$ subbands away from the Fermi energy, and second the hybridization between Pu $6d$ and chalcogenide p and $5f$ bands leads to a hybridization gap. The anomalous lattice constants, which correspond neither to Pu^{2+} nor to Pu^{3+} are consistent with the energy band approach, as is the lattice constant where the transition to Pu^{2+} is expected. Our calculations suggest that Pu has a $5f^{6-x}6d^x$ configuration, where x depends on the lattice parameter, but the sum of $5f$ and $6d$ occupancy is constant. Calculations of the optical conductivity spectra show that there are two optical pseudogaps, one of about 20 meV and one of 0.2 eV. A magnetic phase transition is predicted to occur in the NaCl structure under pressure. When this phase transition is enforced in a magnetic field and takes place before the martensitic transition to the CsCl structure occurs, it is predicted to lead to a giant magnetoresistance of about -85% .

I. INTRODUCTION

The plutonium monochalcogenides display a variety of anomalous physical properties.¹⁻³ Exceptionally, for actinide chalcogenides, they do not order magnetically but are temperature-independent paramagnets.¹ The temperature dependence of the resistivity suggests a complex semiconductor. There is evidence for energy gaps of 0.2 eV, 20 meV,^{1,4} and 3 meV.^{1,2} The precise low-temperature electronic specific-heat coefficient γ is not known, but an extrapolation to zero temperature yielded $\gamma=30 \text{ mJ mol}^{-1} \text{ K}^{-2}$ for PuTe, a very high value for a semiconductor.⁵ On the other hand, x-ray photoemission spectroscopy on PuSe revealed a $5f$ -related intensity directly at the Fermi energy, something that cannot be simply reconciled with a semiconductor.⁶ The induced magnetic form factor is incompatible with Pu^{2+} or Pu^{3+} ions.⁷

The lattice constants of the Pu monochalcogenides are also anomalous. Figure 1 shows the lattice constants of the actinide pnictides and chalcogenides with, for comparison, those of the corresponding rare earths.⁸ They are far too small for divalent ions. There is a $5f$ bonding contribution in the light actinide pnictides and chalcogenides and the maximum bonding occurs for the uranium pnictides. Actinide- $5f$ anion- p bonding is larger early in the series when there are fewer $5f$ -electron states occupied.⁹ The lattice constant of PuTe is consistent with a trivalent Pu ion but the lattice constants of PuSe and PuS are anomalously small.

Two theoretical explanations of the unusual properties of the Pu chalcogenides have been proposed. Brooks¹⁰ carried out self-consistent electronic structure calculations using the Dirac equation in the atomic sphere approximation (ASA) for the Pu monochalcogenides. One of the essential results of that study was that the large spin-orbit (SO) interaction of Pu splits the $5f$ states by approximately 1 eV, so that the Fermi energy (E_F) falls in the gap between the SO-split $5f$ sub-

bands. The Pu chalcogenides were therefore proposed to be relativistic semiconductors.¹⁰ Subsequently Hasegawa and Yamagami¹¹ made self-consistent linearized augmented-plane-wave (LAPW) calculations for PuTe and found it to be semimetallic. The essential difference between the two sets of self-consistent calculations was that the former did not use the combined correction terms to ASA, resulting in an increased energy gap. Wachter *et al.*² suggested that PuTe is an intermediate valence (IV) compound, and that the properties of PuTe should be comparable to those of SmS in the collapsed phase. NaCl-type rare earth and actinide compounds normally make the transition to CsCl structure under pressure. Wachter *et al.* argued that if the f^n-d separation is less than about 1 eV, corresponding to an applied pressure of about 100 kbar, a transition to intermediate valence occurs

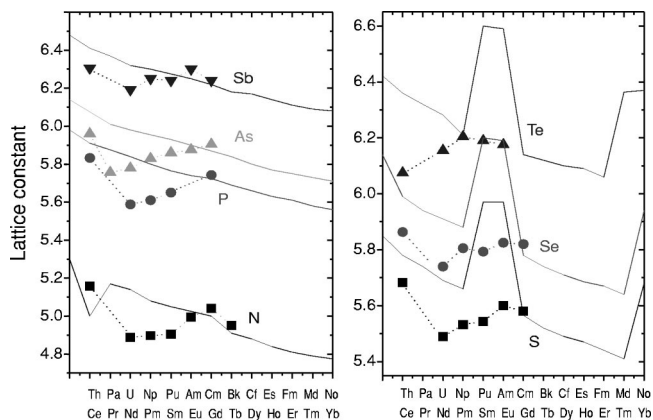


FIG. 1. Lattice constants of the NaCl-type rare-earth and actinide pnictides and monochalcogenides. The lines denote the lattice constants of the rare earths, and the symbols those of the actinides. The lattice constant of ThTe is anomalously small since it forms only in the CsCl structure and shown is the NaCl lattice constant for the same volume.

before the end of a NaCl-CsCl structural transition. While Wachter *et al.*² consider Pu and Sm chalcogenides to be analogs, the latter are semiconducting at ambient pressure and become IV and then trivalent under pressure, whereas the former are proposed to be intermediate valent at ambient pressure. The argument is based upon the high specific-heat γ value and the optical plasma resonance of free carriers, which appear to rule them out as true semiconductors at ambient pressure. The argument is supported by the low bulk modulus, a feature of IV.

Since the theory of IV in rare earths is based upon a localized $4f$ configuration the energy of the $4f$ states is dispersionless in the absence of $4f$ - $5d$ hybridization. If $4f$ - $5d$ hybridization is local at the atom, it must, on parity grounds, be due to nonspherical components of the potential which are small in the region where the $4f$ density is large. If $4f$ - $5d$ hybridization arises from a $4f$ - $5d$ hopping integral, which is more realistic, it is also small as it relies upon $4f$ -electron tunneling. In the former case $4f$ - $5d$ hybridization is constant across the zone, there are no hybridized solutions at the original unhybridized $4f$ energy, and there is always a gap. In the latter case it is possible but unlikely that $4f$ - $5d$ hybridization vanishes somewhere in the zone therefore there should also be a small energy gap. The presence of a small energy gap of the order of meV is therefore evidence supporting IV. In rare earths, since $4f$ - $4f$ electron interaction leads to Russell-Saunders coupling, the SO interaction is the final perturbation to be applied when it forms the total angular momentum and it does not affect the energy gap.

A reasonable starting point for the discussion of the anomalous properties of the Pu monochalcogenides is a detailed knowledge of the electronic structure obtained from self-consistent calculations. In the present paper we report the results of such electronic structure calculations. As particular models have been proposed previously for the electronic structure of PuTe, for which also most experiments were carried out,^{2-5,12} we shall give this compound special attention. We find for the Pu monochalcogenides that the combination of intra-atomic $5f$ - $5f$ and $5f$ -chalcogenide p hybridization is not negligible. The $5f$ bands are dispersive even in the absence of $5f$ - $6d$ hybridization; therefore $5f$ - $6d$ hybridization alone cannot be responsible for the gap at the Fermi energy as in rare earths. We find, in contrast, that the SO interaction is large in the actinides and that it affects their properties to first order, leading to the formation of $5f_{5/2}$ and $5f_{7/2}$ bands. When these bands hybridize with other conduction bands the SO splitting produces a quasigap of just less than 1 eV between the SO-split bands. The $5f_{5/2}$ -derived bands hold just six electrons and are filled in the Pu monochalcogenides. The Pu valence is noninteger and, since the $5f_{5/2}$ -derived bands are almost filled, the electrons contained in them are almost localized.

The results of the band-structure calculations are presented in Sec. II. We find the Pu monochalcogenides to be semimetallic, with tiny Fermi surface portions. This finding is consistent with recent resistivity and optical measurements.^{12,13} There is a quasigap in the band structure, which becomes a real band gap for the lattice constant corresponding to the Pu²⁺ ion. From the calculated total energy and band structures, we then consider the possible phase transitions that could take place and compute the optical reflectiv-

ity spectra. A particular point that we address is the possibility of a magnetic phase transition in the Pu monochalcogenides in an applied magnetic field under pressure. Such a phase transition leads to drastically altered transport properties, and we predict that such a phase transition is accompanied by a giant magnetoresistance.

II. SELF-CONSISTENT BAND-STRUCTURE CALCULATIONS

A. The electronic ground state

Our band-structure calculations are based upon the local spin-density approximation (LSDA) to density-functional theory. The LSDA Kohn-Sham equation has been solved using a relativistic version of the augmented-spherical-wave (ASW) method.¹⁴ In this energy-linearized band-structure scheme first the scalar-relativistic Kohn-Sham equations are solved and then the SO interaction is included in a second variational procedure in every self-consistent iteration step. The potential is treated in the spherical approximation, and combined correction terms are used. In practice, the results of this approach are indistinguishable from calculations based on the Dirac equation. For the exchange-correlation potential we have chosen the parametrization of von Barth and Hedin.¹⁵ The sphere radii used in the calculations were determined by minimizing the charge transfer between the two atoms, which gives sphere radii similar to those obtained from minimizing the Hartree-Coulomb energy. In particular, we have verified that the calculated energy bands are insensitive to reasonable changes of the relative sphere radii. The reciprocal space integrations were carried out using 243 special k points in 1/16th part of the Brillouin zone. Test calculations have been performed also with 646 special k points, but no detectable changes of the band structure could be observed. The core states have been relaxed within every self-consistent iteration step. The Pu $6p$ states are treated as core states.

Figure 2 shows the calculated energy bands of PuS, PuSe, and PuTe, computed for the experimental lattice constants, i.e., 5.530 Å, 5.793 Å, 6.190 Å, for PuS, PuSe, and PuTe, respectively.^{8,13} The quotients of the Pu and chalcogenide sphere radii used in the calculations are 1.180, 1.122, and 1.037, for PuS, PuSe, and PuTe, respectively. For all three chalcogenides, there are clearly two sets of flat bands, one set above and the other set below the Fermi energy with a separation of about 1 eV (see also Refs. 10 and 11). These sets of bands are primarily $5f$ in character and the splitting between them is due to the SO interaction.

We have verified the influence of the SO interaction by multiplying the SO interaction for the $5f$ states by a constant prefactor equal to 0.2, 1.0, and 2.0. The calculated densities of state (DOS) of PuS for the three cases are shown in Fig. 3. The pseudogap, which leaves a small DOS at the Fermi energy, disappears when the prefactor is set equal to 0.2 to reduce the spin-orbit interaction by a factor of 5, and when the magnitude of the spin-orbit interaction is doubled there is a real band gap. In the latter case, with a gap between the $5f_{5/2}$ - and $5f_{7/2}$ -derived bands six valence electrons fill both the bonding and antibonding orbitals of the $5f_{5/2}$ bands. In the former case, where there is no gap, there is a group of fourteen $5f$ bands to be filled and the six electrons enter the

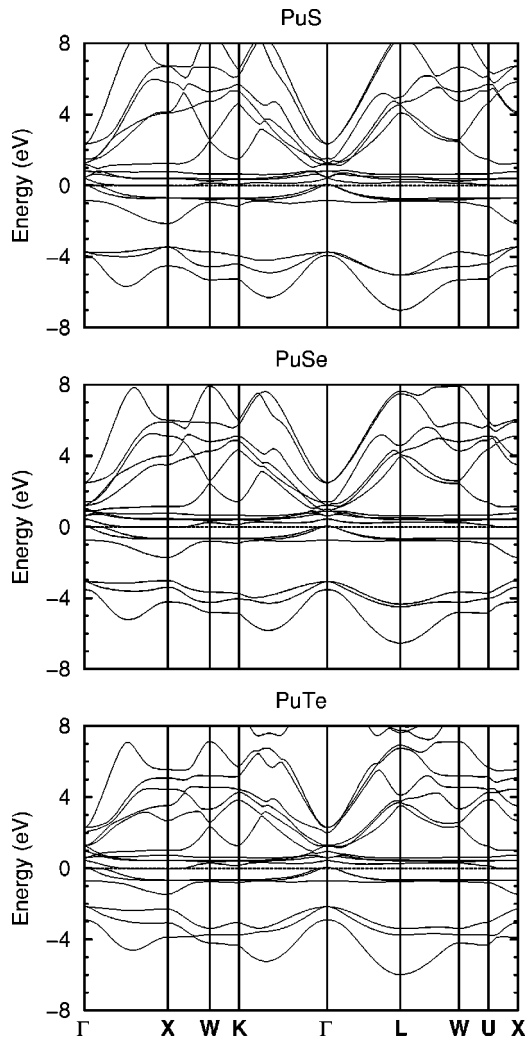


FIG. 2. Calculated energy bands of PuS, PuSe, and PuTe at ambient lattice constant. The Fermi energy is at 0 eV.

bonding bands, leaving the antibonding bands empty. Occupation of antibonding bands increases the lattice constant, and since this occupation increases with spin-orbit interaction, the $5f$ spin-orbit interaction can increase the lattice constant when the $5f$ occupation is about six—a situation realized in the plutonium chalcogenides.

The following broad picture of the Pu monochalcogenides in the NaCl structure emerges. The chalcogenide p bands are completely filled. These are the three filled bands extending from about -7 eV to about -3 eV for all three compounds. The chalcogenide anions are thus in the $2-$ ionic state. Note, that the chalcogenide p bands shift up in energy going from the sulfide to the telluride. This is the normal behavior, related to the increase of the lattice parameter, which was also found for the uranium monochalcogenides.¹⁶ Above E_F there are mostly the Pu $6d$ bands. The bands of primarily $5f$ character are thus placed energetically in between the chalcogenide p bands and the $6d$ bands, which are separated at the Γ point by an energy of about 4 eV. The plutonium $5f$ bands hybridize with the $6d$ bands. In the absence of SO splitting of the $5f$ states the hybridized $5f$ - $6d$ states straddle the Fermi energy, and the chalcogenides would, in this case, be magnetic metal since the Stoner criterion is easily fulfilled just as in uranium and neptunium chalcogenides. In the pres-

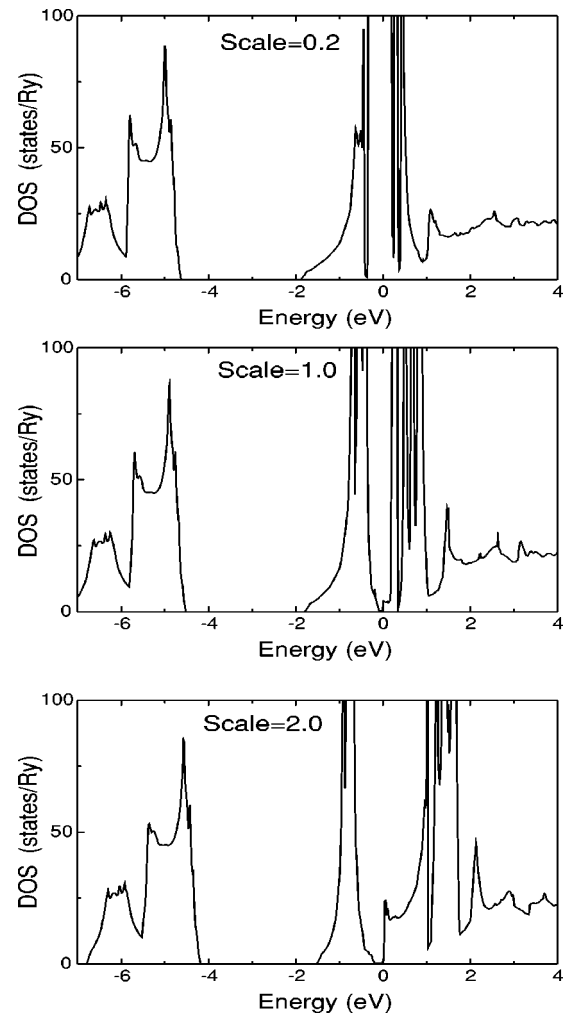


FIG. 3. The pseudogap in the density of states (DOS) of PuS as a function of the scaled spin-orbit interaction. The fully relativistic calculation is labeled by “Scale=1.0.” The pseudogap vanishes when the spin-orbit interaction is made 5 times smaller (“Scale=0.2”).

ence of the SO interaction, there is, however, a large pseudogap due essentially to a splitting between the $5f_{5/2}$ -derived bands and the $5f_{7/2}$ -derived bands of about 1 eV. In these compounds there are 12 valence electrons per formula unit, six of which fill the chalcogenide p bands. The remaining six electrons are nearly enough to fill the $5f_{5/2}$ -derived bands, except for a small portion of these bands at the Γ point. Close to the X point there is the next energy band, which also crosses E_F . The Fermi energy lies thus in a pseudogap, yet there are two small hole Fermi surface pockets about the Γ point and a small electron Fermi surface at the X point. The result is that the Pu monochalcogenides are calculated to be compensated metals, having a tiny Fermi surface. Next to the SO splitting of the $5f$ subbands there is a second, more subtle, mechanism that is responsible for the formation of the quasigap. The Pu $5f$ and $6d$ bands hybridize such that a hybridization gap is formed where these bands would otherwise cross. In Fig. 2 it can be seen that for all three chalcogenides there is at the X point the lowest energy band of the hybridized $5f$ - $6d$ complex. This band originates from a band of $6d$ character above E_F at the Γ point. The hybridization of this band with the SO-split

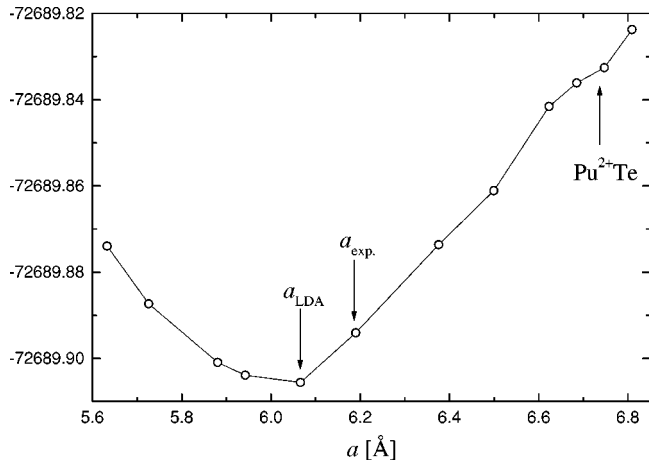


FIG. 4. Calculated total energy of PuTe as a function of lattice constant. The arrow at 6.72 Å indicates the lattice constant for which Pu is expected to have the Pu^{2+} valency.

$5f$ -derived bands is such that instead of band crossing a quasigap is formed along Γ - X . One of the hybridized bands becomes very flat and squeezed on the Fermi energy from above. Below we shall examine the formation of the hybridization-related pseudogap in detail as a function of the lattice constant, which sensitively modifies the f - d hybridization.

The band structure of other actinide monochalcogenides is similar to that of PuS, PuSe, and PuTe, but with the Fermi energy falling below the quasigap and the $5f_{5/2}$ -derived bands partially unfilled, leading to normal metallic behavior. It is therefore the position of E_F relative to the overall band structure that makes the Pu monochalcogenides unique. We have also studied, therefore, the NaCl-type Am monpnictides (for which there is little experimental data), since they are isoelectronic with the Pu monochalcogenides. Although the p -derived valence bands in the pnictides are closer to the conduction bands than in the chalcogenides, the electronic structure is found to be similar. The Fermi energy is again at the top of the $5f_{5/2}$ -derived conduction bands and we find these compounds to be semimetallic when the $5f_{5/2}$ electrons are delocalized. The latter condition is most likely to be fulfilled for AmN, which has an anomalously small lattice constant.

B. The ground-state energy and lattice constant

The calculated total energy of PuTe as a function of lattice constant is shown in Fig. 4. The calculated energy minimum corresponds to a lattice constant of 6.07 Å, which is about 2% less than the measured lattice constant of 6.19 Å. Within the LSDA, a deviation of 2% of the experimental lattice constant is normal, as is also the fact that the calculated lattice constant is smaller. The latter occurs because the LSDA has a tendency to overbind, i.e., make the bond distances shorter. The correct prediction of the lattice parameter is a strong indication that the LSDA electronic structure approach is applicable to describe the anomalous properties of the Pu chalcogenides. Wachter *et al.* have examined the anomalous lattice parameter of PuTe by comparing it to the parameters that are expected (from the ionic radii) for Pu^{2+} and Pu^{3+} .² The lattice parameter expected for PuTe with

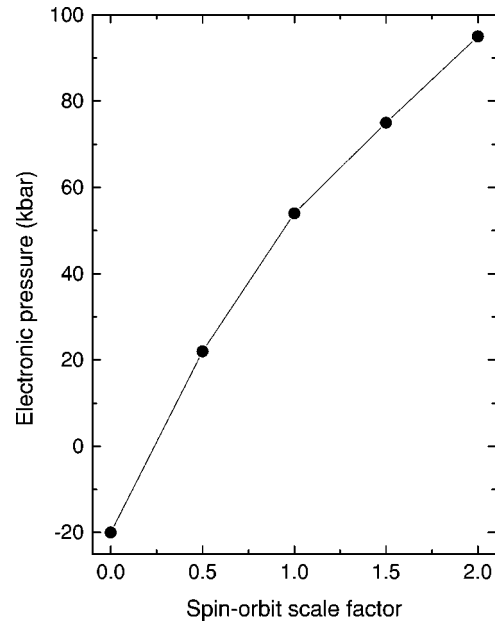


FIG. 5. The change in electronic pressure of PuS as a function of the spin-orbit scaling factor, for a fixed value of lattice constant. The calculation for zero spin-orbit coupling corresponds to the scaling factor 0.0, while the normal relativistic calculation corresponds to 1.0.

divalent Pu is 6.72 Å. Our calculated lattice parameter is much smaller than the divalent PuTe lattice parameter, consistent with the observation that Pu is not in the divalent state.

A lattice constant less than that expected from a localized $5f$ configuration may be attributed to $5f$ bonding, whereas a lattice constant greater than that expected for a normal itinerant system is at least partially explained by the effect of SO interaction. This effect is illustrated in Fig. 5, which shows the calculated electronic pressure (or derivative of the total energy with respect to volume) as a function of SO scaling factor. Since SO coupling splits the $5f$ bands into $5f_{5/2}$ and $5f_{7/2}$ bands the center of all the $5f$ bands is not affected, but the preferential filling of the $5f_{5/2}$ increases the electronic pressure by 80 kbar, which corresponds to a change in lattice constant of 2%. The SO interaction has little effect upon the contribution of other states to the pressure. The fact that the $5f$ contribution to the electronic pressure, and thereby the lattice constant, changes so much with SO coupling constant is therefore due to the filling of the $5f_{5/2}$ -derived bands.

As the lattice constant is increased the $5f$ - $5f$, $5f$ - $6d$, and $5f$ - p hybridization decreases. In order to understand the effect of this hybridization and its dependence upon lattice constant it is useful to start from the extreme case of pure $5f$ bands. Pure SO-split $5f$ bands separate into $5f_{5/2}$ and $5f_{7/2}$ bands. If the SO splitting is very large the intra-atomic hybridization between the $5f_{5/2}$ and $5f_{7/2}$ components is small, the result being that the $5f_{5/2}$ bands are very narrow. Hybridization within the $5f_{5/2}$ states is determined by the expansion of tails of the $5f_{5/2}$ orbitals at a given Pu site about other Pu sites. The multipole expansion of the $5f$ orbitals results in wave functions at the other site with angular momenta obtained by adding an angular momentum of up to $2l=6$ to the $j=5/2$ angular momentum. The addition of angular momenta

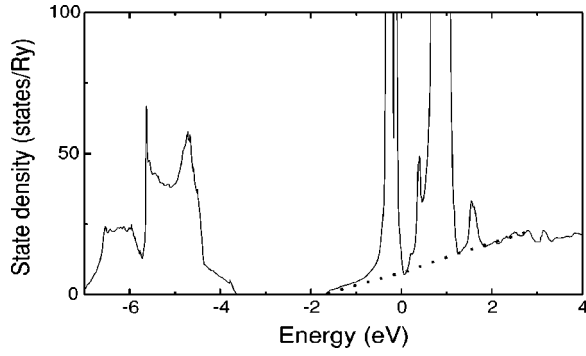


FIG. 6. The state density of PuS with hybridization between the Pu $5f$ states and $6d$ states and sulfur p states removed. The s - p - d free-electron background is the dotted line.

restricts the expanded multipoles to $l=17/2, \dots, 7/2$. There is therefore no $5f_{5/2}$ component and the interatomic $5f_{5/2}$ - $5f_{5/2}$ hybridization vanishes. The SO interaction in Pu is not large enough to drive this extreme case and the $5f_{5/2}$ bands obtain width through hybridization with the $5f_{7/2}$ bands. Hybridization in general decreases with increasing lattice constant, but the above-mentioned effect amplifies the influence of lattice constant upon the width of the $5f_{5/2}$ bands and the size of the pseudogap. In Fig. 6 we have plotted the state density of PuS with hybridization between the $5f$ and $6d$ and sulfur p states removed. This was done by setting the appropriate structure constant blocks to zero in a model calculation. The hybridization gap is removed and the s - p - d states produce a free-electron-like background state density with the SO-split $5f$ state density superimposed. Thus it is the combination of SO splitting of the $5f$ states and the hybridization with d and p states that produces a pseudogap.

The $5f$ - $5f$ and $5f$ - $6d$ hybridization is sensitively dependent upon the lattice constant. In Fig. 7 the changes of the quasigap in PuTe are shown for three expanded lattice constants. For the experimental lattice constant there is the one band that, without hybridization, would extend from above E_F at the Γ point to below E_F at the X point (see Fig. 2). Particularly this band changes as the lattice is expanded: its position in energy at X increases rapidly, whereas minimal changes occur in the bands at K - Γ - L . Note that although this band changes substantially, the quasigap itself remains stable. An examination of the orbital occupation numbers further illustrates how the electronic structure changes with the lattice constant: Only the relative Pu $5f$ and $6d$ occupation numbers are continuously altered, their sum remaining constant, which relates to the anion 2-valency staying constant. The Pu configuration is thus $5f^{6-x}6d^x$, where x is the $6d$ occupation number, the value of which decreases with increasing lattice constant. Near the experimental lattice constant x is approximately 0.4–0.5. We note, though, that the LSDA approach probably tends to overestimate hybridization.

When the lattice is expanded to a constant of 6.75 Å no bands cross the Fermi energy; see Fig. 7. At this point the $5f_{5/2}$ bands are filled, the $5f_{7/2}$ bands are empty, and PuTe is a semiconductor. If there were no SO interaction the compound would remain a metal. The lattice constant of about 6.72 Å at which PuTe becomes a semiconductor corresponds

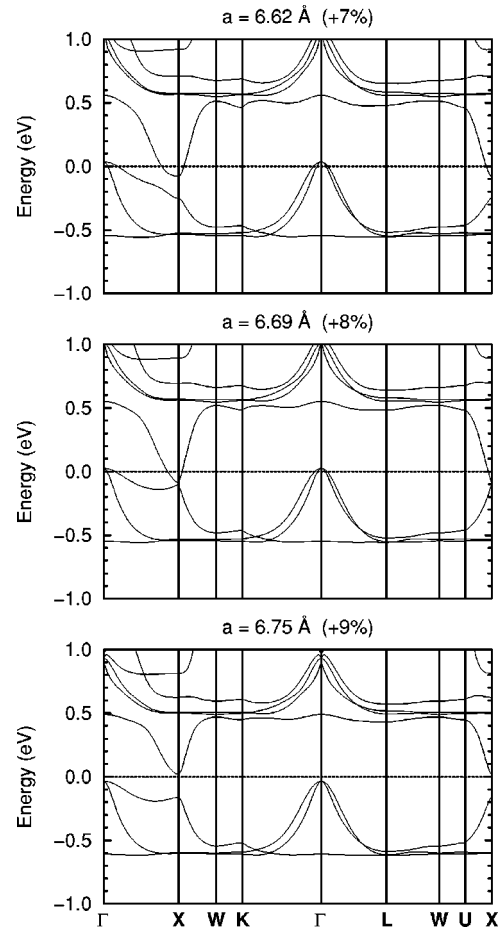


FIG. 7. Energy bands of PuTe in the vicinity of the Fermi energy for lattice constants that are 7%, 8%, and 9% expanded with respect to the experimental lattice constant.

closely to the expected lattice constant for a divalent Pu ion.² The total energy around this lattice constant shows an anomaly¹⁷ (see Fig. 4) that would lead to an increased compressibility for lattice constants just less than 6.72 Å. We note, with respect to the discussion of which model description is applicable to PuTe, that the LSDA approach thus predicts the lattice parameter at which the transition to Pu²⁺ is expected. We also note that the occurrence of a real semiconductor gap in expanded PuTe is reminiscent of the conductivity behavior of SmS.¹⁸ SmS is, at ambient pressure, a semiconductor with Sm in the divalent state, which makes the transition to the IV metallic state under pressure. However, in contrast to the theory of localized f configurations, we emphasize once more that although the $5f_{5/2}$ bands are filled the energy dispersion of these $5f$ bands is an order of magnitude greater than for $4f$ states.

C. Optical properties

A more detailed examination of the quasigap upon physical properties is facilitated by an examination of the optical properties. To calculate the optical spectrum we have employed the linear-response expression for the optical conductivity $\sigma(\omega)$:

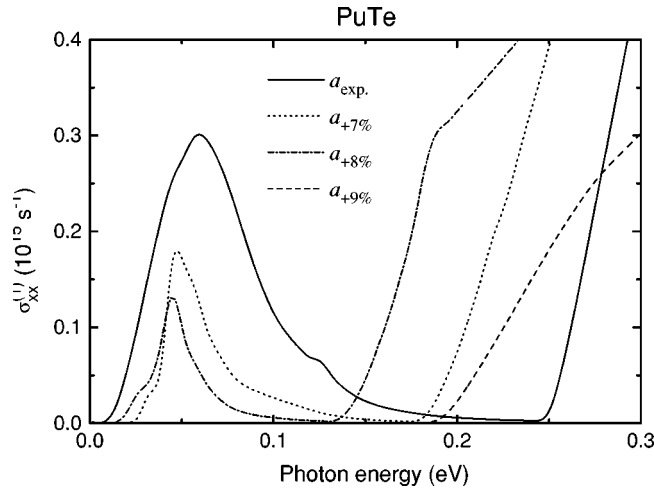


FIG. 8. Calculated optical conductivity $\sigma_{xx}^{(1)}$ of PuTe for the experimental lattice constants, and for three lattice constants, 7%, 8%, and 9% expanded, at about which the semimetal-semiconductor transition occurs.

$$\sigma(\omega) = \frac{-ie^2}{3m^2\hbar V_{uc}} \sum_{\mathbf{k}} \sum_{nn'} \frac{f(\epsilon_{n\mathbf{k}}) - f(\epsilon_{n'\mathbf{k}})}{\omega_{nn'}(\mathbf{k})} \times \frac{|\Pi_{n'n}(\mathbf{k})|^2}{\omega - \omega_{nn'}(\mathbf{k}) + i/\tau}, \quad (1)$$

where $f(\epsilon_{n\mathbf{k}})$ is the Fermi function, $\hbar\omega_{nn'}(\mathbf{k}) \equiv \epsilon_{n\mathbf{k}} - \epsilon_{n'\mathbf{k}}$, the energy difference of the Kohn-Sham energies $\epsilon_{n\mathbf{k}}$, and τ^{-1} is the lifetime parameter, which is included to describe the finite lifetime of excited electron states. The $\Pi_{n'n}(\mathbf{k})$ are the matrix elements of the relativistic momentum operator. Details of the computation of σ and Π can be found in Refs. 19 and 16.

The calculated absorptive part of the interband optical conductivity is shown in Fig. 8 in the photon energy range 0–0.3 eV as a function of lattice constant close to the semimetal-semiconductor transition. For comparison we also included the spectrum calculated for the ambient lattice constant. For the latter lattice constant two optical gaps are present, one of about 20 meV and a larger one of about 0.2 eV. The smaller one slightly increases with increasing lattice constant. The spectral intensity at 0.05 eV decreases with increasing lattice constant, until at a lattice constant of 6.72 Å, corresponding to the semimetal-semiconductor transition, this intensity and the smaller gap completely disappear, leaving only the semiconducting gap of 0.2 eV. The large gap corresponds to the pseudogap between the $5f_{5/2}$ - and $5f_{7/2}$ -derived bands, whereas the smaller gap of about 20 meV corresponds to the separation of the two bands at the Γ point (see Fig. 7). In the calculation of σ we have not taken the intraband contribution to the optical conductivity into account. The small Fermi surface leads to a Drude-type intraband conductivity. Very similar spectra have been calculated for PuS and PuSe, and thus we shall not show these separately.

The reflectivity spectrum of PuTe was recently measured by Mendik *et al.*³ From the calculated optical conductivity the theoretical reflectivity can straightforwardly be obtained and compared to experiment. In Fig. 9 the experimental and

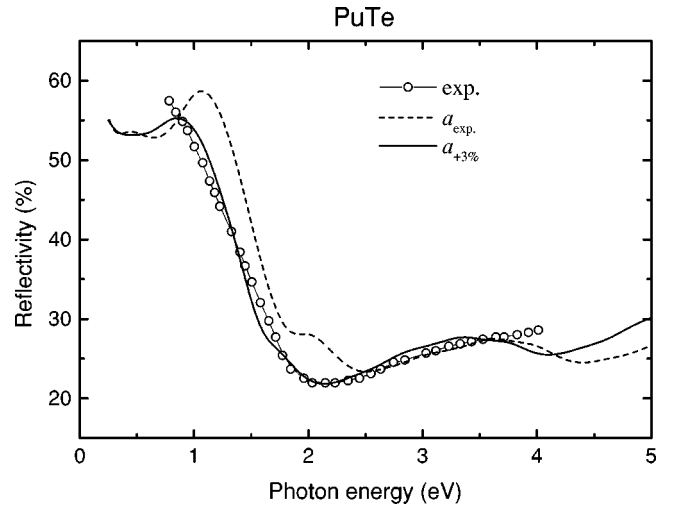


FIG. 9. Calculated and measured reflectivity of PuTe. The theoretical spectra are obtained for the experimental lattice constant, $a = 6.19$ Å, and for a 3% expanded lattice constant. The experimental data (○) are from Ref. 3.

calculated reflectivities are shown. A constant lifetime parameter $\hbar\tau^{-1} = 0.2$ eV has been applied in the calculation. The reflectivity calculated for the ambient lattice constant is in overall agreement with experiment, except for a small peak at 2 eV, which is not observed in the experiment. As the LSDA approach tends to too strong a hybridization, we expect that the $5f$ - $6d$ hybridization can be reduced by a small lattice expansion. The influence of a 3% lattice expansion is also shown in Fig. 9: the agreement with experiment becomes excellent. This result definitely supports the LSDA description of the electronic structure. Very recently it has become clear from several computational investigations of optical and magneto-optical spectra that the appropriate description of the electronic structure will provide an accurate explanation of the measured spectra.^{20–22}

D. Semiconducting properties and specific heat

As mentioned before, three effective energy gaps have been determined from the temperature-dependent resistivity.^{1,2,4} Our energy-band calculations predict, however, the Pu monochalcogenides at ambient pressure to be semimetallic, due to the existence of tiny Fermi surfaces. A scrupulous analysis of the available data shows, in our opinion, that the Pu monochalcogenides are not truly semiconducting materials. The smallest, low-temperature gap that has been identified is of the order of 0.5 meV to 3 meV.^{1,2} Yet, the low-temperature resistivity is not correspondingly high. We may, for example, compare to the thoroughly studied compound SmB_6 , which is an IV semiconductor with an established energy gap of 4–5 meV (see Ref. 18). The resistivity of SmB_6 rises appreciably at low temperatures, to about 1 Ωcm , a value that is 1000 times higher than the measured low-temperature resistivity of PuTe.¹ Furthermore, the occurrence of a Drude-like edge in the near-infrared reflectivity spectrum has been considered as an indication of free carriers.^{3,13} Also, photoemission spectroscopy revealed a $5f$ -related peak in the vicinity of E_F .⁶ Due to final-state effects the photoemission spectrum need not be in a one-to-

one correspondence with single-particle state densities; nonetheless, an energy gap at E_F could not be detected. From these data we infer that the Pu monochalcogenides are semimetallic, in agreement with the band-structure result. The experimentally observed resistivity behavior is unusual,^{1,12} but as shown above, there is a gap of about 20 meV in the optical conductivity spectrum. While an optical gap is not straightforwardly related to a thermal gap, it is nevertheless reasonable to anticipate that a signature of the optical gap becomes visible in the resistivity.

A very recent investigation of the resistivity behavior of PuTe under pressure revealed an anomalous upturn of the low-temperature resistivity.¹² Under pressure conduction and valence bands normally broaden, which should thereby decrease any semiconducting gap. Obviously the resistivity of PuTe does not follow the standard behavior. The quasigap in PuTe arises in a usual manner from the SO interaction and the $5f$ - $6d$ hybridization, which we expect to be the reason of the pressure-increased resistivity. To examine this conjecture we have calculated the zero-temperature conductivity σ_0 , which is given by

$$\sigma_0 = \frac{e^2}{3m^2 V_{uc}} \sum_{n\mathbf{k}} \tau |\Pi_{nn}(\mathbf{k})|^2 \delta(\epsilon_{n\mathbf{k}} - E_F), \quad (2)$$

as follows from Eq. (1) for $\omega=0$. The relaxation time τ is unknown and may result from various complex many-particle interactions. We adopt here the constant relaxation time approximation, which is sufficient for a qualitative understanding. From Eq. (2) we find that the resistivity of PuTe increases by 53% in going from the 3% expanded lattice to the ambient lattice constant. An even further decrease of lattice parameter, from the 3% expanded lattice to a 3% contracted lattice, leads to a resistivity increase of 141%. The anomalous resistivity increase in PuTe is thereby indeed confirmed as a peculiarity of the quasigap. Here we have chosen the 3% expanded lattice constant in order to mimic best the calculated electronic structure of PuTe to the experimental electronic structure, in accordance with the conclusion derived from the reflectivity spectrum.

The specific-heat coefficient measured for PuTe is approximately 30 mJ/mol K².⁵ From the DOS at the Fermi energy we obtain theoretical specific-heat coefficients of $\gamma \approx 5$ –6 mJ/mol K² for all three chalcogenides. These γ 's are thus about 5 times smaller than the measured γ . We note, however, that there is the one very flat band close to the Fermi energy (see Fig. 2). The flatness of this particular band causes a peak in the DOS at energies up to 4–5 meV above E_F . This high DOS would correspond to a γ of 20 to 30 mJ/mol K², depending somewhat on the energy distance to E_F . At finite temperatures the effect of the peak would be to increase the theoretical γ over the 0 K value. In combination with an anticipated many-body enhancement factor of about 2 for actinides, the measured specific heat could then be accounted for.

E. Magnetic form factor

The induced magnetic form factor of PuTe has been measured by Lander *et al.*⁷ There can be a significant difference in the induced magnetic form factor of a paramagnetic metal

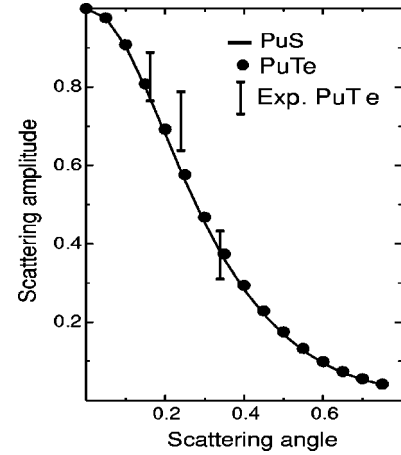


FIG. 10. The calculated induced magnetic form factors of PuS and PuTe. The solid line depicts the calculated form factor of PuS, and the dots that of PuTe. The vertical bars give the experimental data points for PuTe after Ref. 7.

and that of a magnetic metal when the magnetic electrons are itinerant and the SO interaction is large.²³ When a light actinide is magnetic and the spin density large, the SO interaction induces a large orbital moment antiparallel to the spin moment, leading to a magnetic form factor for which the orbital effects are visible as a long tail,²⁴ such as in PuSb.⁷ In uranium metal, in contrast, the induced form factor falls off rapidly with scattering vector, the explanation being that the induced spin density is so small that the SO interaction has less effect than the applied field, which tends to align orbital and spin moments parallel. In fact, the effects of the applied field and SO interaction tend to cancel, leading to a smaller induced orbital moment parallel to the spin moment, which is difficult, if not impossible, to observe. We have calculated the induced form factors for PuS and PuTe by applying small magnetic fields to the results of a paramagnetic calculation and verified that both the induced spin and orbital moments were proportional to the applied field. For small applied fields the spin and orbital moments are parallel and the orbital moment is a factor of 5 larger than the spin moment. The resulting magnetic form factors, which are shown in Fig. 10, decreases monotonically with scattering vector, indicating that there is no cancellation of spin and orbital moments in PuS or PuTe. The calculated form factor is in good agreement with the experimental result for PuTe (see Fig. 10) from which the same conclusions were drawn.⁷ Otherwise, when the spin and orbital magnetic moments are antiparallel and of about the same magnitude, the general shape of the form factor is different, and it must resemble the form factor of UN,²⁴ which is typical for most actinide compounds. In the present calculation the induced moment contains a Pauli contribution since the DOS at the Fermi energy is not zero but also a significant Van Vleck contribution since higher-lying states are mixed into the ground state by the applied field.

F. Possible magnetic phase transition

The above-discussed properties of the Pu monochalcogenides are all based on paramagnetic electronic structure calculations, extended with a small applied magnetic field

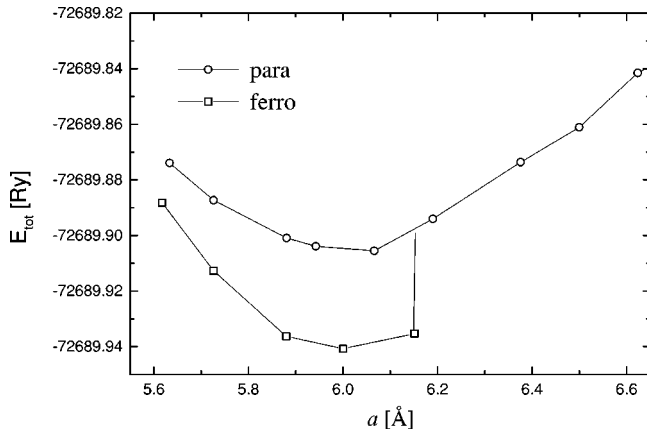


FIG. 11. Total energy versus lattice parameter for PuTe, calculated for both paramagnetic and ferromagnetic PuTe in the NaCl crystal structure.

only to compute the magnetic form factor. In our calculations we observe a peculiarity for all three Pu monochalcogenides: Quite abruptly, as a function of the lattice constant, a transition to a ferromagnetic state is found. This ferromagnetic state is predicted to have a lower total energy than the paramagnetic state. In Fig. 11 the ferromagnetic and paramagnetic total energies of PuTe as a function of lattice parameter are shown. The onset of ferromagnetic order is calculated to occur close to $a=6.15$ Å. At the experimental lattice constant of 6.19 Å, a self-consistent calculation that started from a ferromagnetic state converges to a zero moment solution. Otherwise, the moments in the ferromagnetic state are not small: the spin moment is about $5.0\mu_B$, and the orbital moment $-2.7\mu_B$, depending on the lattice parameter and the chalcogenide anion. The moments are mainly due to the $5f$ states, the s - p - d states contribute a small spin moment of about $0.3\mu_B$, and an orbital moment of $0.06\mu_B$, both parallel to the respective $5f$ moments. The sudden onset of ferromagnetic ordering seems anomalous.¹⁷ Nothing of this kind has yet been observed experimentally. In view of our above-reported results for the paramagnetic state, which correspond unmistakably to the available experimental data, we are inclined to exclude the possibility that the obtained ferromagnetic state is an artifact of the LSDA energy-band approach. We remark, with respect to the computed ferromagnetic ground state, first, that we did not try to find an antiferromagnetic state that could eventually have an even lower total energy. Second, it is known that the LSDA approach has a tendency to prefer the ferromagnetic state over the paramagnetic one. However, since the total energy of the ferromagnetic state is not nearly degenerate with that of the paramagnetic one, we consider it unlikely that the ferromagnetic state would not be the lower-in-energy state. So far a magnetic state has not been observed in the Pu monochalcogenides. As the agreement with experimental data is best for the 3% expanded lattice parameter, we anticipate that an experimental detection of ferromagnetism needs to be done in pressure experiments. A complication inherent to observing a magnetic phase transition is the structural NaCl-CsCl phase transition, which occurs in the Pu monochalcogenides under pressure, and is rather sluggish.^{25,26} One of the questions would therefore be if a possible magnetic phase transition would occur before the end of the structural phase tran-

sition. Recently the temperature-dependent resistivity of PuTe was measured under pressure, but these initial efforts did not detect an additional phase transition.¹² A better chance to detect magnetic order might be in PuS, because in PuS the NaCl-CsCl transition occurs beyond 60 GPa,²⁷ whereas in PuSe and PuTe it occurs at about 35 GPa, and 15 GPa, respectively.^{13,25,26} On the basis of first-principles calculations we cannot adequately address the question whether the structural phase transition would occur first, because of our current band-structure method, which uses the spherical-potential approximation.¹⁴ A full-potential approach would be required to calculate accurately the NaCl-CsCl transition pressure.

The origin of the onset of magnetism in the Pu monochalcogenides does not rest in the Stoner criterion. The DOS at E_F is, in the paramagnetic state, not so high that it becomes reduced in the ferromagnetic state. The DOS in the ferromagnetic state is, on the contrary, similar or somewhat higher. Instead, to understand the magnetic phase transition, we note once more that our calculations indicate that a continuous shift of the $5f$ occupancy to the $6d$ occupancy takes place under pressure. This f - d occupation shift corroborates with the magnetic transition. It is therefore instructive to begin with PuTe at an expanded lattice constant, which corresponds to a paramagnetic Pu $5f^6 6d^0$ configuration. Under pressure, the Pu configuration shifts to $5f^{6-x} 6d^x$, where the $5f$ occupation approaches a $5f^5$ occupancy at high enough pressure. For Pu in the latter configuration, magnetic ordering is energetically more favorable. The initially spin-degenerate $5f_{5/2}$ band becomes spin split, and part of the exchange-split bands are shifted through the Fermi energy. The Fermi surface of the ferromagnetic Pu monochalcogenides is thus much bigger than the tiny portions present in the paramagnetic state. Using again Eq. (2), and adopting for simplicity the constant relaxation-time approximation, we can calculate the field-induced magnetoresistivity, from

$$\left(\frac{\Delta\rho}{\rho}\right) = \frac{\rho(B) - \rho(0)}{\rho(0)}, \quad (3)$$

with $\rho(B)$ and $\rho(0)$ the resistivity in the ferromagnetic and paramagnetic states, respectively. The calculated magnetoresistivities are enormous: -83% , -87% , and -87% , for PuS, PuSe, and PuTe, respectively. Such giant values of the magnetoresistivity are sometimes observed for certain uranium compounds, like, e.g., UNiGa, where -87% was measured.²⁸ However, for the uranium compound the metamagnetic transition that is induced by the applied magnetic field is from an antiferromagnetic ground state to a ferromagnetic state. In the case of the paramagnetic Pu monochalcogenides the quasigap is destroyed by the field. With respect to the huge resistivity changes accompanying the magnetic transition, we mention that also the resistivity of PuTe in the CsCl phase is much smaller than that of the NaCl phase (Refs. 12 and 29).

III. DISCUSSION AND CONCLUSIONS

The $5f$ SO splitting is larger and $5f$ - $5f$ and $5f$ - d hybridization an order of magnitude larger in the actinides than in the rare earths. We would therefore expect that the basis for model calculations would be better provided by energy-band

calculations than by atomiclike calculations. The detailed calculations presented here already provide a reasonable explanation of many of the anomalous properties of the plutonium monochalcogenides. In particular, the equilibrium lattice constant of PuTe, calculated using the LSDA, corresponds quite closely to the measured one, without the necessity for any further assumptions. Also the lattice constant where the transition to Pu²⁺ is expected is nicely reproduced by the LSDA energy-band calculation. The calculated induced magnetic form factor of PuTe is also close to that measured, and the computed, unenhanced, specific-heat coefficients compare reasonably with the measured value for PuTe. The calculated optical reflectivity of PuTe is in good agreement with experiment too, suggesting that at least our calculated electronic structure of a semimetal with a quasigap is essentially correct. The magnitude of the smallest quasigap of about 20 meV in the optical conductivity spectrum is similar to that of the energy gap deduced from low-temperature resistivity measurements. Responsible for the formation of the quasigap is the large SO interaction that splits the Pu 5f_{5/2} and 5f_{7/2} subbands at the Fermi energy, in combination with a hybridization gap being formed by the Pu 5f and 6d bands. The hybridization gap is especially sensitive to modifications of the 5f-5f, 5f-6d, and Pu-chalcogenide *p* hybridizations. As a consequence, the resistivity is calculated to increase under moderate pressure, which is unusual, but in agreement with recent measurements.¹²

Our calculations show that the electronic structure lies very close to an essentially filled set of 5f_{5/2}-derived bands that contain an admixture of *d* states. This suggests a 5f^{6-x}6d^x configuration for Pu. Although such a configuration corresponds to the intermediate valence suggested for the Pu monochalcogenides,^{2,3} there are pertinent differences to the theory of IV developed for rare earths. In the latter, the rare earth 4f bands are dispersionless, which is not the case

for the 5f-derived bands. In addition, the large SO interaction affects the 5f bands to first order. If a localized model were to be made that started from this calculated band structure, the localized states would be Wannier functions constructed from this filled set of bands. Such a set of localized states, which may indeed be required to construct the low-lying excited states, still differs from the localized states used for models of intermediate-valent rare-earth compounds, since SO interaction and 5f-6d hybridization have been included from the outset in the energy-band calculations. In this sense, mixed valence in the actinides must be essentially different from mixed valence in the rare earths.

Previously, two phase transitions were discussed for the Pu monochalcogenides: the transition from the Pu²⁺ valent state to mixed valence,^{2,3} and the structural NaCl-CsCl transition under pressure.^{13,25,26} Our total-energy calculations predict the possibility of a third phase transition under pressure, that from a paramagnetic state to a ferromagnetic state. Although a magnetic phase transition has not yet been observed, we believe that under pressure, at a reduced lattice constant, this should be possible. Also, our energy-band calculations predict the Pu monochalcogenides to be semimetallic, with small Fermi surface portions. A further test of this proposed electronic structure would be de Haas-van Alphen measurements of the Fermi surface.

ACKNOWLEDGMENTS

We have benefited from discussions with V. Ichas, G. H. Lander, J. Schoenes, P. Wachter, L. Havela, T. Gouder, H. Eschrig, and J. M. Fournier. Part of this work has been performed while P.M.O. and T.K. were at the Max-Planck-Research Group "Theory of Complex and Correlated Electron Systems." Financial support from the Max-Planck Society, and from the State of Saxony (under Contract No. 4-7541.83-MP2/301) is gratefully acknowledged.

*Present address: Institute of Solid State and Materials Research, P.O. Box 270016, D-01171 Dresden, Germany.

¹J.M. Fournier, E. Pleska, J. Chiapusio, J. Rossat-Mignod, J. Rebizant, J.C. Spirlet, and O. Vogt, *Physica B* **163**, 493 (1990).

²P. Wachter, F. Marabelli, and B. Bucher, *Phys. Rev. B* **43**, 11 136 (1991).

³M. Mendik, P. Wachter, J.C. Spirlet, and J. Rebizant, *Physica B* **186-188**, 678 (1993).

⁴E. Gómez Marín, Ph.D. thesis, University of Grenoble, 1997.

⁵G.R. Stewart, R.G. Haire, J.C. Spirlet, and J. Rebizant, *J. Alloys Compd.* **177**, 167 (1991).

⁶J.R. Naegele, F. Schiavo, and J.C. Spirlet (unpublished); J.R. Naegele and L. Havela (unpublished).

⁷G.H. Lander, J. Rebizant, J.C. Spirlet, A. Delapalme, P.J. Brown, O. Vogt, and K. Mattenberger, *Physica B* **146**, 341 (1987).

⁸J. M. Fournier and R. Troć, in *Handbook on the Physics and Chemistry of the Actinides*, edited by A.J. Freeman and G.H. Lander (North-Holland, Amsterdam, 1985), Vol. 2, p. 29.

⁹M.S.S. Brooks and D. Glötzel, *Physica B* **102**, 51 (1980).

¹⁰M.S.S. Brooks, *J. Magn. Magn. Mater.* **63&64**, 649 (1987).

¹¹A. Hasegawa and H. Yamagami, *J. Magn. Magn. Mater.* **104-107**, 65 (1992).

¹²V. Ichas, J. Rebizant, and J.C. Spirlet (unpublished).

¹³C. Abraham, U. Benedict, and J.C. Spirlet, *Physica B* **222**, 52 (1996).

¹⁴A.R. Williams, J. Kübler, and C.D. Gelatt, *Phys. Rev. B* **19**, 6094 (1979).

¹⁵U. von Barth and L.A. Hedin, *J. Phys. C* **5**, 1692 (1972).

¹⁶T. Kraft, P.M. Oppeneer, V.N. Antonov, and H. Eschrig, *Phys. Rev. B* **52**, 3561 (1995).

¹⁷We do not use a fixed radial grid inside the atomic spheres, but radial grids that are reevaluated for every sphere radius. The anomaly in the total energy in Fig. 4, and the discontinuity in the ferromagnetic total energy in Fig. 11, are thus not due to discontinuous changes of the number of radial grid points with the sphere radius.

¹⁸P. Wachter, in *Handbook on the Physics and Chemistry of the Rare Earths*, edited by K.A. Gschneidner, Jr., L. Eyring, G.H. Lander, and G.R. Choppin (North-Holland, Amsterdam, 1994), Vol. 19, p. 177.

¹⁹P.M. Oppeneer, T. Maurer, J. Sticht, and J. Kübler, *Phys. Rev. B* **45**, 10 924 (1992).

²⁰A. Delin, P.M. Oppeneer, M.S.S. Brooks, T. Kraft, B. Johansson, and O. Eriksson, *Phys. Rev. B* **55**, R10 173 (1997).

²¹P.M. Oppeneer, M.S.S. Brooks, V.N. Antonov, T. Kraft, and H. Eschrig, *Phys. Rev. B* **53**, R10 437 (1996).

- ²²P.M. Oppeneer, A.Y. Perlov, V.N. Antonov, A.N. Yaresko, T. Kraft, and M.S.S. Brooks, *J. Alloys Compd.* **271-273**, 831 (1998).
- ²³A. Hjelm, O. Eriksson, and B. Johansson, *Phys. Rev. Lett.* **71**, 1459 (1993).
- ²⁴M.S.S. Brooks and P.J. Kelly, *Phys. Rev. Lett.* **51**, 1708 (1983).
- ²⁵S. Dabos-Seignon, U. Benedict, S. Heathman, and J.C. Spirlet, *J. Less-Common Met.* **160**, 35 (1990).
- ²⁶M. Gensini, E. Gehring, S. Heathman, U. Benedict, and J.C. Spirlet, *High Press. Res.* **2**, 347 (1990).
- ²⁷T. le Bihan, S. Heathman, and J. Rebizant, *High Press. Res.* **15**, 387 (1997).
- ²⁸V. Sechovský, L. Havela, L. Jirman, W. Ye, T. Takabatake, H. Fujii, E. Brück, F.R. de Boer, and H. Nakotte, *J. Appl. Phys.* **70**, 5794 (1991).
- ²⁹B. Johansson, O. Eriksson, M.S.S. Brooks, and H.L. Skriver, *Inorg. Chim. Acta* **140**, 59 (1987).